

TITLE
*ASP Conference Series, Vol. **VOLUME**, **PUBLICATION YEAR***
 EDITORS

Pair Creation at Shocks: Application to the High Energy Emission of Compact objects

P.O. Petrucci

Osservatorio Astronomico di Brera, Milano, Italy

G. Henri², G. Pelletier²

Laboratoire d'Astrophysique, Grenoble, France

Abstract. We investigate the effect of pair creation on a shock structure. Actually, particles accelerated by a shock can be sufficiently energetic to boost, via Inverse Compton (IC) process for example, surrounding soft photons above the rest mass electron energy and thus to trigger the pair creation process. The increase of the associated pair pressure is thus able to disrupt the plasma flow and possibly, for too high pressure, to smooth it completely. Reversely, significant changes of the flow velocity profile may modify the distribution function of the accelerated particles, modifying consequently the pair creation rate. Stationary states are then obtained by solving self-consistently for the particle distribution function and the flow velocity profile. We discuss our results and the application of these processes to the high energy emission and variability of compact objects.

1. Introduction

The high energy emission observed in compact objects like AGNs or X-ray binaries requires the existence of high energy particles. Shocks being particularly attractive particle acceleration sites, they are generally believed to occur in the central region of these objects. In these cases however, the presence of important radiation fields necessitate to take into account particles-photons interactions in the shock region.

If some works have already studied particles acceleration at shocks including radiative cooling processes (Webb et al., 1984; Drury et al., 1999) we have investigated the effect of pair creation on the shock structure (Petrucci et al., hereafter P00). Particles accelerated by the shock can effectively be sufficiently energetic to boost, via Inverse Compton (IC) process for example, surrounding soft photons above the rest mass electron energy and thus enable to generate pairs. Consequently, the increase of the pair pressure may be able to modify the plasma flow and eventually, for too high pressure, to smooth it completely.

We describe here the geometry of the (toy) model we use (cf. Fig 1). We present the basic equations and the main results of this model. We then briefly discuss its application to the high energy emission and variability of compact objects.

2. The Toy Model

The schematic view of our toy model is plotted in Fig. 1. We suppose the existence of a thermal supersonic plasma undergoing an adiabatic **non-relativistic shock**. It is supposed to be **embedded in an isotropic external soft photon field**. We assume the presence of a magnetic field \vec{B}_o , parallel to the shock normal, frozen in the plasma and slightly perturbed by Alfvén waves. We suppose the magnetic energy to be in equipartition with the particles kinetic energy so that, in each part of the shock, the Alfvén wave speed is equal to the flow speed. Particles are then scattered by Alfvén waves through pitch angle scatterings, gaining energy through the **first order Fermi process** when crossing back and forth the shock discontinuity. We also suppose the magnetic perturbations to have sufficiently small amplitudes so that we can treat the problem in quasilinear theory using the **Fokker-Planck formalism**. Finally, we suppose the **plasma pressure to be dominated by the pressure of the relativistic particles**. In this case, the flow velocity profile makes already a smooth transition between the up and downstream region but acceleration still occurs.

2.1. The Geometry

The shock location: We assume a 1D geometry. It means that the different parameters characterizing the flow are supposed to be homogeneous in each section perpendicular to the x axis. This is a relatively good approximation in the central parts of the shock where the border effects are negligible. We suppose the shock to be located in $x = 0$ (cf. Fig. 1). During numerical integrations, this will be ensured by imposing that the flow velocity $u(x)$ possesses an inflection point in $x = 0$ that is:

$$\left. \frac{\partial^2 u}{\partial x^2} \right|_{x=0} = 0 \quad (1)$$

The acceleration region: A particle of Lorentz factor γ will interact with the shock if it is located within about one diffusion length $L_D(\gamma) = D_{xx}/u$ (where D_{xx} is the spatial diffusion coefficient) from the shock. On the other hand it will be cooled (by Inverse Compton process) on a cooling length scale $L_{cool}(\gamma)$. L_D and L_{cool} are increasing and decreasing functions of γ respectively. There thus exists a Lorentz factor γ_c for which:

$$L_D(\gamma_c) = L_{cool}(\gamma_c) = L$$

We will define the acceleration region as the physical space $-L \leq x \leq L$ (hatched region in cf. Fig. 1). Consequently, in this region the **coolings are negligible in comparison to heatings** for particles with $\gamma < \gamma_c$ since for such particles $L_D(\gamma) < L_{cool}(\gamma)$.

In the following we will suppose the spatial diffusion coefficient D_{xx} to be independent of the energy of the particles and it will be simply written D .

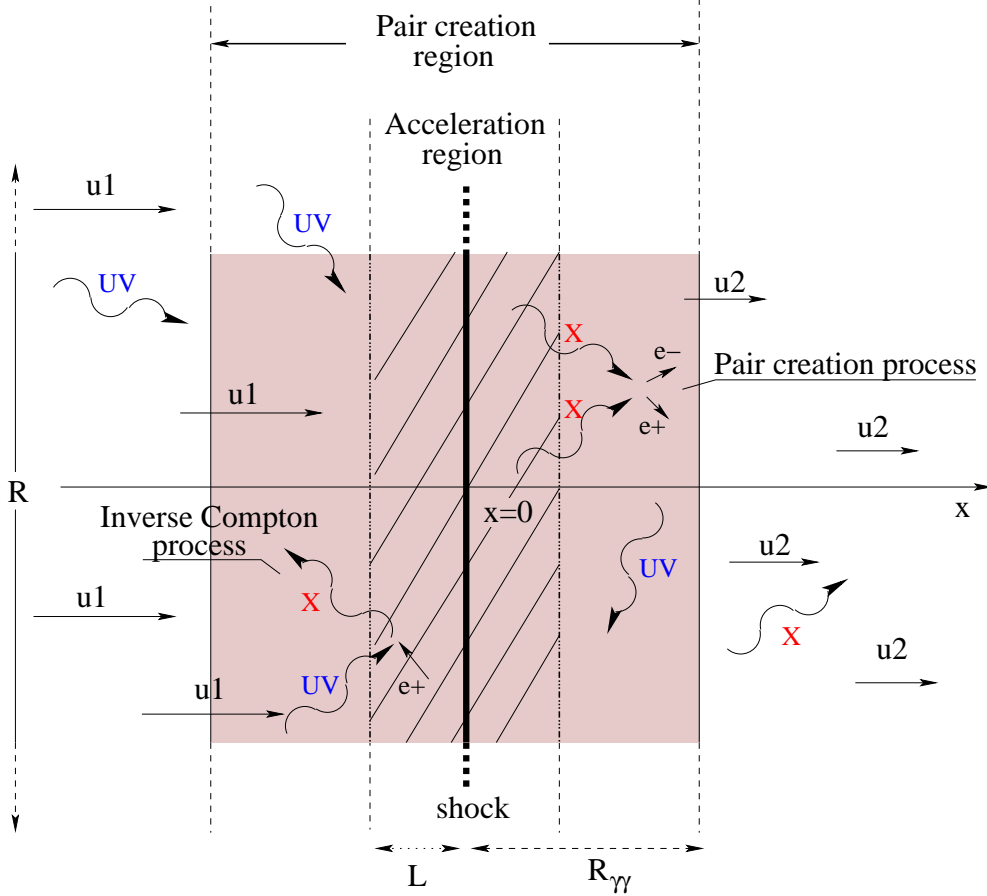


Figure 1. The geometry of our (toy) model. The shock discontinuity is represented by the bold line. The hatched region is the acceleration region and the pair creation one is filled in pink. Particles are represented by straight arrows and photons by warped ones (in blue for surrounding soft, i.e. UV, photons, and in red, high energy, i.e. X-ray, photons). Scales are not respected.

The pair creation region: Particles accelerated in the shock will produce high energy photons by scattering, via Inverse Compton process (IC), the external soft photons. These high energy photons will interact with themselves to produce pairs on a length scale $R_{\gamma\gamma}$. Typically we have:

$$R_{\gamma\gamma} \simeq \frac{R}{1 + \tau_{\gamma\gamma}}$$

where R is the typical size of the shock (cf. Fig. 1). This expression take into account the photon-photon depletion for $\tau_{\gamma\gamma} \gg 1$ and the geometrical dilution of the X-ray photon density, far from the shock, which upperlimits the pair creation region size to roughly the shock size R . We will define the pair creation

region by $-R_{\gamma\gamma} \leq x \leq +R_{\gamma\gamma}$.

We assume the pair pressure creation rate to be constant in the pair creation region (that is for $-R_{\gamma\gamma} \leq x \leq R_{\gamma\gamma}$) and null outside. This assumption may be supported by the fact that magnetic turbulence, supposed to be present to scatter particles, is a useful process to isotropize and homogenize the plasma in the vicinity of the shock in very small time scale

The “effective” compression ratio: The definition of the compression ratio like the ratio between the far upstream and downstream flow velocity is rather unsatisfactory in our case since it will not give a real estimate of the velocity change experienced by a relativistic particle in the vicinity of the shock, where the particle distribution is principally built. We will thus define an “effective” compression ratio, noted simply r , as the ratio between the upstream velocity in $-10L$ and the downstream velocity in $+10L$. We have checked that in the case of a strong shock without pairs, this definition still gives a compression ratio very near the expected value (in a plasma dominated by relativistic particles) of 7.

2.2. Important energetic al thresholds

The acceleration threshold: Only particles having a Larmor radius r_L comparable to the wavelength of the Alfvén spectrum will undergo scatterings (Jokipii, 1976; Lacombe, 1977) and thus will go back and through many times across the shock. In $e^- - p^+$ plasma as those we deal with, the non-relativistic protons limit the Alfvén waves spectrum to wavelength greater than $2\pi V_A / \omega_{cp}$ (ω_{cp} is the cyclotron pulsation of the protons in a magnetic field B , and V_A is the Alfvén velocity). Consequently there exists a lower Lorentz factor for a relativistic lepton to be accelerated in a shock:

$$\gamma > \gamma_{min} = \frac{m_p}{m_e} \frac{V_A}{c}$$

In the more general case γ_{min} is at least of the order of a few. We will admit that pre-accelerator processes exist (like magnetic reconnection, whistler) to bring particles above γ_{min} . Consequently, since particles annihilate preferentially for $\gamma \simeq 1$ (Coppi & Blandford, 1990), **we will neglect the annihilation process in the shock region.**

The pair creation threshold: We will suppose for simplicity that the external soft photon field is mono-energetic with a mean photon energy ϵ_s (in $m_e c^2$ unit). Thus, on average, a soft photon scattered by a lepton of Lorentz factor γ will be boosted, via IC, to an energy $\epsilon \simeq \frac{4}{3} \gamma^2 \epsilon_s$ (Rybicki & Lightman, 1979). The high energy photon produced will be able to generate a pair electron-positron if at least:

$$\epsilon > 2m_e c^2 \text{ i.e. } \gamma \geq \left(\frac{3m_e c^2}{2\epsilon_s} \right)^{1/2} = \gamma_{th}$$

We assume $\gamma_{th} > \gamma_{min}$ so that particles have to be accelerated in the shock to initiate the pair creation process.

2.3. The particle distribution

The spectral index: It can be shown that the solution of the evolution equation of the particle distribution function including the pair creation process (cf. Eq. (5)), still has a energy power law dependence, as it is effectively the case without pairs (P00). The spectral index s (here s is the spectral index of the spatially integrated distribution function of the particles $n(\gamma) \propto \gamma^{-s}$) keeps also the same expression in function of the compression ratio i.e.:

$$s(r) = (r + 2)/(r - 1). \quad (2)$$

For plasma dominated by relativistic pressure, the compression ratio is necessarily smaller than 7 so that $s(r)$ is larger than 1.5.

The high energy cut-off: Since we take into accounts the cooling, a high energy cut-off in the particle distribution must necessarily appear at a Lorentz factor γ_c where heating and cooling balance (Webb et al., 1984). Since we suppose that particles cool via inverse Compton process (assuming that the external soft photon density is homogeneous in the shock region) and that they are accelerated by the first order Fermi process, the maximum Lorentz factor γ_c achievable by the acceleration process may be written as follows (P00):

$$\gamma_c \propto \frac{1}{l_s} \frac{u_1}{c} \frac{r - 1}{3(1 + r^2)} \quad (3)$$

where l_s is the soft compactness ($l_s = \frac{L_{soft}\sigma_T}{4\pi R m_e c^3}$, m_e being the electron mass and L_{soft} the external soft radiation luminosity) and u_1 the upstream flow velocity.

From these different remarks, we will assume that the particle distribution has a cut-off power law shape, i.e.:

$$n(\gamma) \propto \gamma^{-s} \exp\left(-\frac{\gamma}{\gamma_c}\right) \quad (4)$$

3. The basic kinetic equations

As previously said, we suppose the existence of a magnetic field \vec{B}_o , perpendicular to the shock front and slightly perturbed by Alfvén waves. The particles are thus scattered by these waves through pitch angle scattering (Jokipii, 1976; Lacombe, 1977) and can cross the shock front several times before escaping unless they are rapidly cooled by radiative processes. During these scatterings, the particle gain energy through the well known first order Fermi process. We also suppose the magnetic perturbations to have sufficiently small amplitudes so that we can treat the problem in quasilinear theory using the Fokker-Planck formalism. Besides we assume that, in each part of the shock front, the scattering is sufficient for the particle distribution to be nearly isotropic. With these different assumptions, and when first order Fermi process just as radiative losses

and pair creation/annihilation are taken into account, the particles distribution function $f(p, x)$ must verify the following equation :

$$\begin{aligned} \frac{\partial f}{\partial t} + u \frac{\partial f}{\partial x} &= \frac{1}{3} \frac{\partial u}{\partial x} p \frac{\partial f}{\partial p} + \frac{1}{p^2} \frac{\partial b p^4 f}{\partial p} + \frac{\partial}{\partial x} D \frac{\partial f}{\partial x} \\ &+ \mathbf{C}_\pm(f) + \mathbf{D}_\pm(f). \end{aligned} \quad (5)$$

The three first terms of the right member correspond to the first order process, the radiative losses (b being > 0 , the detailed expression of b in the case of Inverse Compton cooling can be found in P00) and the spatial diffusion respectively, $\mathbf{C}_\pm(f)$ is the pair creation rate and $\mathbf{D}_\pm(f)$ the annihilation one. This equation is essentially the equation of the cosmic-ray transport originally given by Parker (1965), Skilling (1975 and references therein) except for the addition of the radiative losses and the pair processes.

Since we suppose that the shocked plasma pressure is dominated by the pressure of the relativistic particles, we can deduce, from Eq. 5, the hydrodynamic equation linking pairs (through their pressure) and the flow velocity $u(x)$, that is (in stationary state):

$$u \frac{\partial P_{\text{rel}}}{\partial x} + \frac{4}{3} P_{\text{rel}} \frac{\partial u}{\partial x} = \frac{\partial}{\partial x} D_{xx} \frac{\partial}{\partial x} P_{\text{rel}} + \dot{Q}_{\text{rel}} + \dot{P}_\pm \quad (6)$$

where \dot{Q}_{rel} is the pressure loss rate due to radiative losses and \dot{P}_\pm the pair pressure creation rate.

A way to solve Eq. (6) is to integrate it between $-\infty$ and $+L$. In this case, we can neglect the cooling during the integration. Indeed, even if for $x \leq -L$ particles do not interact with the shock, we have assumed that some processes apply and balance coolings so that particles are injected above the resonance threshold γ_{\min} . On the other hand, in the shock region (that is $-L \leq x \leq L$), we have seen in section 2.1 that the coolings are negligible, in comparison to heatings, for particles with a Lorentz factor smaller than γ_c (the case of the majority of the particles). Besides, we can also neglect the annihilation since it occurs mainly at low energy, i.e. for particles with Lorentz factor $\gamma \simeq 1$ (cf. Coppi & Blandford, 1990), whereas we assume $\gamma \geq \gamma_{\min}$. In these conditions, and with the assumption that the pair creation is homogeneous in the region $-R_{\gamma\gamma} < x < +R_{\gamma\gamma}$ (meaning \dot{P}_\pm roughly constant) and null outside (meaning $\dot{P}_\pm = 0$), the integration of Eq. (6) between $-\infty$ and L , combined with the momentum conservation equation, gives (in reduced units):

$$\frac{\partial \tilde{u}}{\partial \tilde{x}} = \frac{7}{6} (1 - \tilde{u}) \left(\frac{1}{7} - \tilde{u} \right) + \Pi \left(1 + \frac{\tilde{x}}{\tilde{R}_{\gamma\gamma}} \right) \quad (7)$$

where the reduced variables are defined as followed:

$$\tilde{u} = \frac{u}{u_1} \quad (8)$$

$$\tilde{x} = \frac{x}{L} \text{ and } \tilde{R}_{\gamma\gamma} = \frac{R_{\gamma\gamma}}{L} \quad (9)$$

$$\Pi = \frac{\dot{P}_\pm R_{\gamma\gamma}}{\rho u_1^3}. \quad (10)$$

Π is the ratio of the pair luminosity (the pair power density integrated on the “1D” volume $R_{\gamma\gamma}$) to the kinetic energy flux of the flow. This parameter will play an important role in the evolution of the shock profile as we will see in the following. We can anticipate that a large value of Π will be certainly unfavorable to the formation of the shock. It means that all the kinetic energy of the upstream flow will be dissipated in pair creation processes.

4. Shock disappearance

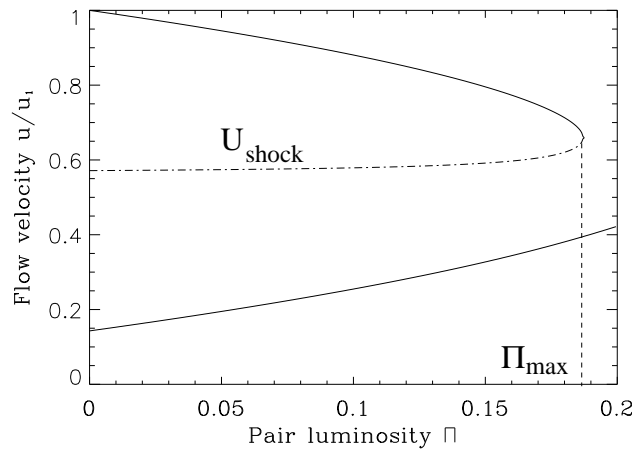


Figure 2. Plot of the 3 solutions of Eq. (11) versus Π for $\tilde{R}_{\gamma\gamma} = 50$. The flow velocity \tilde{u}_{shock} at the shock location, i.e. in $x = 0$ is plotted in dashed line. There is a maximal value of Π , Π_{\max} , above which only one real solution exists. Consequently, for $\Pi > \Pi_{\max}$ the shock disappears.

The shock still exists as long as Eq. (1) is verified. Combining with Eq. (7), Eq. (1) becomes:

$$\begin{aligned} \left. \frac{\partial^2 \tilde{u}}{\partial \tilde{x}^2} \right|_{x=0} = P(\tilde{u}) &= 49\tilde{u}^3 - 84\tilde{u}^2 + (39 + 42\Pi)\tilde{u} \\ &- 24\Pi + 18\frac{\Pi}{\tilde{R}_{\gamma\gamma}} - 4 = 0 \end{aligned} \quad (11)$$

Since $P(\tilde{u})$ is a third degree polynomial, it possesses in general 3 real solutions which depends obviously on Π and $\tilde{R}_{\gamma\gamma}$. They have been plotted in Fig. 2 in function of Π for $\tilde{R}_{\gamma\gamma}=50$. Of course, for Π going to zero, the three branches of solution converge respectively to the well-known results $\tilde{u}=1/7$, $4/7$ and 1 corresponding to the values without pair creation. By continuity, the flow velocity

at the shock location will follow the second branch noted \tilde{u}_{shock} on the figure (plotted in dashed line). **It appears that for a given value of $\tilde{R}_{\gamma\gamma}$ it exists**

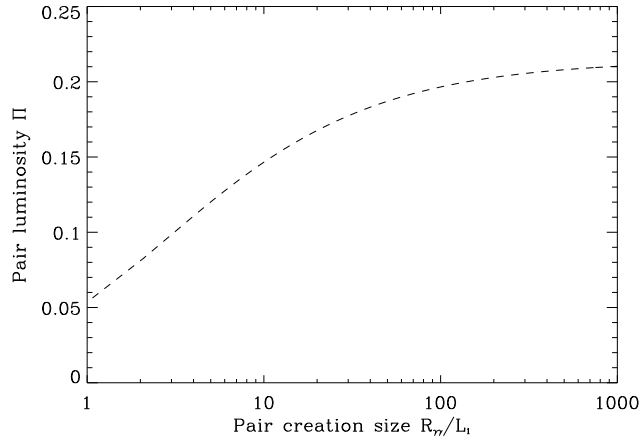


Figure 3. Curve Π_{max} vs. $\tilde{R}_{\gamma\gamma}$. We see that Π_{max} is upperlimited by ~ 0.2 .

a maximal value Π_{max} of Π above which there is only one real solution which still verifies Eq. (11). The unphysical discontinuity of the flow velocity at the shock location for $\Pi = \Pi_{max}$ means simply that the shock can not exist anymore.

The transition between 3 to 1 real solution of Eq. (11) happens when the following conditions are satisfied:

$$P(\tilde{u}) = 0 \quad (12)$$

$$P'(\tilde{u}) = 0 \quad (13)$$

The resolution of this system of equations gives thus a relation between Π_{max} and $\tilde{R}_{\gamma\gamma}$:

$$\Pi_{max} = \frac{3}{14} - \frac{1}{14} \left(63 \frac{\Pi_{max}}{\tilde{R}_{\gamma\gamma}} \right)^{2/3} \quad (14)$$

We have reported the corresponding function $\Pi_{max}(\tilde{R}_{\gamma\gamma})$ in Fig. 3. We see that Π_{max} is a increasing function of $\tilde{R}_{\gamma\gamma}$ meaning that the larger the pair creation region the larger the pair power we need to kill the shock. However, we see from Eq. (14) that Π_{max} is necessarily smaller than $3/14 \simeq 0.20$ meaning that **at most 20% of the kinetic energy flux of the upstream flow transformed in pairs is sufficient to suppress the shock discontinuity**.

We have reported in Fig. 4, different shape of the polynomial $P(\tilde{u})$ and the corresponding flow velocity profiles obtained numerically by solving Eq. (7) for different values of Π (fixing $\tilde{R}_{\gamma\gamma}$ to 10). We have also plotted in Fig. 5, the variation of the compression ratio r (as defined in section 2.1) in function of the pair creation rate Π . As expected, r converge to ~ 1 when Π increases meaning that the acceleration becomes less and less efficient.

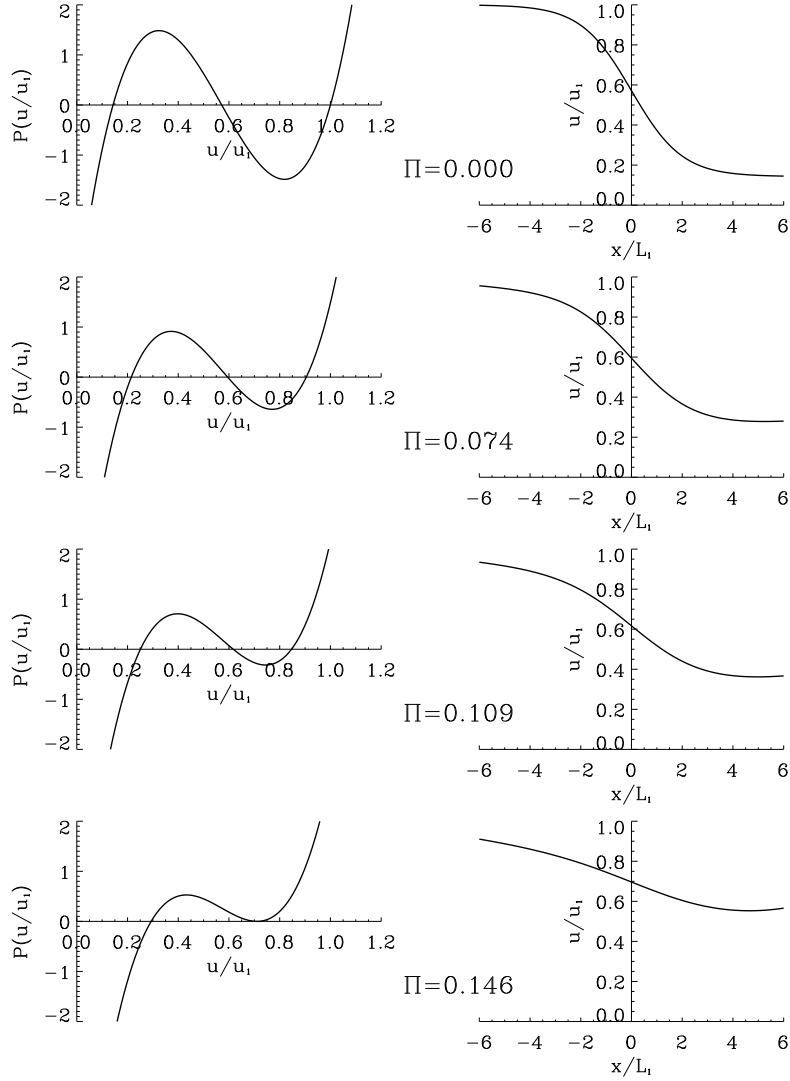


Figure 4. disappearance of a shock due to pair creation. We have taken $\tilde{R}_{\gamma\gamma}=10$ meaning that Π must be smaller than ~ 0.15 (cf. Fig. 3).

5. Stationary states

Up to now, we have supposed that the deformation of the flow profile, due to the pair pressure, does not modify the pair creation rate itself. This is a crude assumption since a change in the velocity profile of the flow will modify the distribution function of the accelerated particles in such a way that the number of particles enable to trigger the pair creation process (i.e. particles with $\gamma \geq \gamma_{th}$)

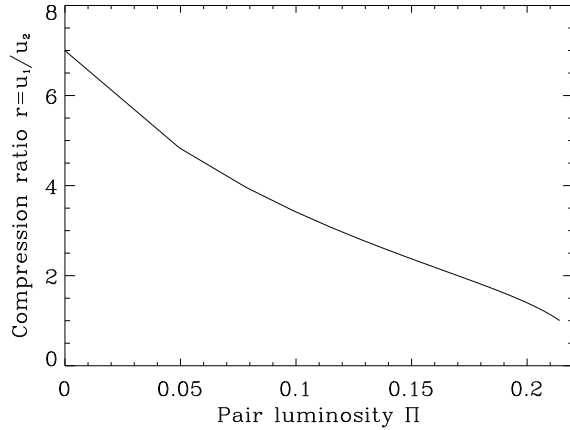


Figure 5. Variation of the compression ratio r in function of the pair luminosity Π for $\tilde{R}_{\gamma\gamma} = 1000$.

may change, modifying consequently the pair creation rate.

From the previous section we have seen that the compression ratio r decreases when the pair creation rate raises (cf. Fig. 5) but reversely if r decreases, the spectral index will increase and the number of high energy particles will decrease, the final effect being a decrease of the pair creation rate. Consequently, we may expect the system to reach, in some conditions, stationary states where hydrodynamics and pair creation effects balance.

5.1. The parameter space

We have studied the stationary states of our toy model by solving self-consistently for the particle distribution function $n(\gamma)$ and the flow velocity profile $u(x)$, the two function $n(\gamma)$ and $u(x)$ being linked through the pair pressure. In stationary states, the system depends on six different parameters: γ_{min} , the minimal Lorentz factor for the particles to be accelerated in the shock (cf. section 2.2), ϵ_s , the external soft photon energy (in unit of $m_e c^2$), u_1 , the upstream flow velocity, \tilde{R} the transverse size of the shock (in unit of the diffusion length L), l_s , the compactness of the external soft photon field (cf. section 2.3) and l_{kin} the kinetic compactness defined as $l_{kin} = \frac{(\rho u_1^3 \pi R^2) \sigma_T}{4\pi R m_e c^3}$. The larger l_s and the larger the cooling of the particles, whereas the larger l_{kin} and the larger the kinetic energy of the upstream flow.

The system is solvable in only some part of the parameter space. It always possesses two solutions: a “pair dominated” (large pair luminosity Π , small compression ratio r) and a “pair free” one (small Π , large r). The latter connects to the trivial solution of the problem i.e. $\Pi = 0$.

5.2. High energy spectra

For a given set of parameters, the system may reach stationary states characterized by a compression ratio r . The spectral index and cut-off of the particle distribution function (Eq. (4)) are then given by Eq. (2) and (3) respectively. Since we have assumed that these particles are cooled by Inverse Compton effect and that their distribution function follows Eq. (4), the emitted energy spectrum is characterized by a cut-off power law shape $F_E \propto E^{-\alpha} \exp \left[- \left(\frac{E}{E_c} \right)^{\frac{1}{2}} \right]$ where α and E_c are simple functions of s and γ_c (Rybicki & Lightman, 1979):

$$\alpha = \frac{s}{2} \quad (15)$$

$$E_c \simeq \frac{4}{3} \gamma_c^2 \epsilon_s m_e c^2 \quad (16)$$

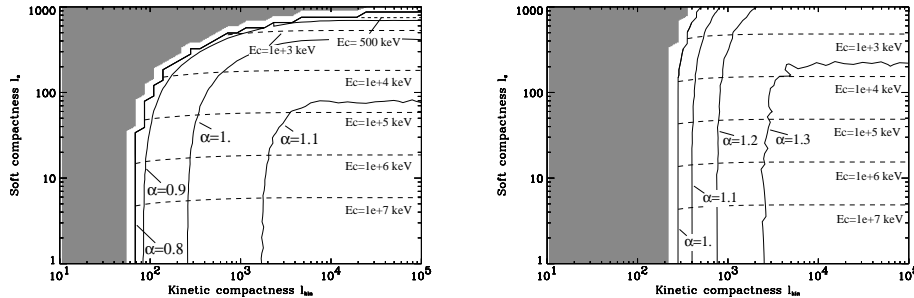


Figure 6. Contour plots of the spectral index α (solid lines) and the high energy cut-off E_c in keV (dashed lines) of the emitted spectrum in the (l_s, l_{kin}) space. The soft photon energy is equal to 10 eV and 600 eV in the left and right plot respectively. The other parameters have been fixed to $\tilde{R} = 10^8$, $\gamma_{min} = 10$ and $u_1/c = 0.1$. In the grayed region there is no stationary state solution.

We have reported in Fig. 6 the contour plot of $\alpha(l_s, l_{kin})$ and $E_c(l_s, l_{kin})$ for two values of ϵ_s (10 and 600 eV which are representative of the typical values of soft photons emitted by an accretion disk around a supermassive and stellar mass black hole respectively). The other parameters have been fixed to $\tilde{R} = 10^8$, $\gamma_{min} = 10$ and $u_1/c = 0.1$. The contours of α and E_c keep roughly the same shape but cover a different region of the parameter space for different parameter sets. In each figure, we can see that:

- The spectral index does not strongly vary between the harder and the softer spectra ($\Delta\alpha \simeq 0.3$). It reaches an asymptotic plateau for low l_s and high l_{kin} . In these conditions, both pair density and high energy cut-off are large so that the pair creation process is saturated. Concerning E_c , following Eqs. (3) and (16), it is inversely proportional to l_s^2 .

- The harder spectra are obtained for large values of l_s or small values of l_{kin} . In both case, the pair efficiency decreases either due to a small value of E_c or a low particle density, that is a low pair production optical depth. To keep the equilibrium between the pair creation effects and the hydrodynamic of the flow, the system has to reach harder spectra to compensate this decrease of the pair creation rate.
- For small l_s , γ_c is very large ($\gg \gamma_{th}$) and its value becomes immaterial. Consequently, Π and r , and thus α become independent of l_s .
- For large l_{kin} , the pair density must be also high to efficiently modify the hydrodynamical profile. The pair creation process is thus saturated meaning that the pair creation rate grows linearly with l_{kin} , i.e. Π , r and thus α become independent of l_{kin} .
- For to large l_s or to small l_{kin} , the system cannot reach sufficient hard states to keep in equilibrium and no high pair density stationary state can exist any more. The system can only be in the trivial pair free state (i.e. $r = 7$ and $\Pi = 0$).

We interpret the differences between the two plots of Fig. 6 as follows. The increase of ϵ_s favors the pair creation process. Thus, for given values of l_s and l_{kin} , the spectral index is larger. The high energy cut-off E_c increases mainly because of its dependence on ϵ_s (cf. Eq. (16)), γ_c keeping roughly constant (cf. Eq. (3)).

5.3. Annihilation line

The presence of pairs should give a signature as an annihilation feature at ~ 511 keV. We will show that this feature is not expected to be strong in our model. Here, we have supposed the existence in the shock region of pre-accelerating processes bringing leptons to the sufficient energy (i.e. $\gamma > \gamma_{min}$ with γ_{min} of the order of a few, cf section 2.2) for resonant scattering off magnetic disturbances. Since the annihilation process occurs mainly at low energy, i.e. for particles with Lorentz factor $\gamma \simeq 1$ (cf. Coppi & Blandford 1990), it occurs mainly far downstream, where the pairs created in the shock can cool down. The annihilation line luminosity is thus at most equal to the pair rest mass luminosity. As shown in section 4, the pair luminosity Π is itself limited and is necessarily smaller than $\sim 20\%$ of the X-ray/γ-ray luminosity, i.e. $\Pi < \Pi_{max} \simeq 0.2$ (assuming that the total kinetic energy of the upstream flow is transformed in radiation). Besides, for $\Pi \simeq 0.2$, the compression factor is very small, of the order of unity, resulting in a very steep X-ray spectra. When hydrodynamics feedback is taken into account, the pair luminosity may be well below this theoretical limit of 20%. An X-ray spectral photon index ~ 2 (as those generally seen in Seyfert galaxies) requires a compression ratio $r \sim 3\text{--}4$. Such values of r require values of Π smaller than $\simeq 10\%$ (cf. Fig 5).

Assuming a steady state, pairs annihilate at the same rate as they are produced. Π/γ_{min} gives then an upper limit of the annihilation line luminosity. We thus expect the luminosity of the annihilation radiation to be smaller than few percent of the total high energy radiation, which is quite compatible with

the non observation of strong annihilation lines in this class of Seyfert galaxies as shown by the best upper limit observed in Seyfert galaxies with the OSSE satellite (Johnson et al. 1997).

5.4. Variability

For some values of external parameters, as suggested by Fig. 6, no high pair density solution can exist in stationary states. So only the pair free solution (i.e, with $\Pi = 0$) exists. The system is not expected to be variable with a constant set of parameters and variability can only occur with a variation of one of them. An interesting possibility would be to consider a possible feedback of the relativistic plasma to the soft compactness: in the reillumination models for instance (Collin, 1991; Henri & Petrucci, 1997), the soft photons are produced by the reprocessing of the primary X-ray emission. An increase of the pair plasma density will increase the X-ray illumination and thus the soft compactness. Fig. 6 shows that in some cases, the change of l_s make the system switch to pair free solution which will stop the reillumination and bring the system back to pair rich solutions. Limiting cycles could thus occur. We intend to further investigate this possible effect under astrophysically relevant conditions.

6. Conclusion

In the present paper, we have studied the effect of pair creation, via high energy photon-photon interaction, on a shock structure, where the high energy photons are produced via IC by the particles accelerated by the shock itself. The problem is highly nonlinear since pairs can modify the shock profile through their pressure and, mutually, a change of the shock hydrodynamics can decrease or increase the pair production rate.

We have shown that for a given size of the pair creation region, it exist a maximal value of the pair creation rate above which the shock cannot exist anymore. When the hydrodynamical feedbacks on the pair creation process are neglected, a pair power of at most 20% of the upstream kinetic power is sufficient to kill the shock. This constraint can fall to few percents in stationary states where pair creation and hydrodynamical effects balance. We thus do not expect the presence of strong annihilation lines. We also obtain spectral parameters in rough agreement with the observations.

We suggest also a possible variability mechanism if the soft photon compactness depends itself on the pair density of the hot plasma, such as expected in reillumination models.

In the model presented here, the cooling of particles is due to the IC process on external soft photons. However, particles may also cool on soft photon they produce by synchrotron process when spiraling around the magnetic field lines (the so-called synchrotron-self-compton process, SSC). In this case the cooling will also depend on the particle distribution function. We may expect that the addition of the SSC process would allow to obtain stationary states with harder

spectra than those we obtained here, since the additional synchrotron cooling would be compensate by a stronger acceleration, i.e. a larger compression ratio r . The detailed study of this problem is left to future work.

Acknowledgements: POP acknowledges a grant of the European Commission under contract number ERBFMRX-CT98-0195 (TMR network "Accretion onto black holes, compact stars and protostars").

References

Coppi P. & Blandford, R. D. 1990, MNRAS, 245, 453
 Drury, L. O. .., Duffy, P. , Eichler, D. & Mastichiadis, A. 1999, A&A, 347, 370
 Henri, G. & P.O. Petrucci, 1997, A&A, 326, 87 1999, Astroparticle Physics, 11, 347
 Johnson, N. 1997, American Astronomical Society Meeting, 190, 2005
 Jokipii, J. R. 1976, ApJ, 208, 900
 Jones, F. C. 1994, ApJS, 90, 561
 Lacombe, C. 1977, A&A, 54, 1
 Pelletier, G. & Roland, J. 1984, Ap&SS, 100, 351
 Petrucci P.O., Henri G. & Pelletier, G. 2000, A&A submitted
 Rybicki, G. B. & Lightman, A. P. 1979, New York, Wiley-Interscience, 1979.
 Webb, G. M., Drury, L. O. & Biermann, P. 1984, A&A, 137, 185